ChemComm

COMMUNICATION

View Article Online
View Journal | View Issue



Cite this: *Chem. Commun.*, 2017, 53, 881

Received 24th October 2016,
Accepted 2nd December 2016

DOI: 10.1039/c6cc08515f

www.rsc.org/chemcomm

# Highly porous N-doped graphene nanosheets for rapid removal of heavy metals from water by capacitive deionization†

Lianjun Liu,[a] Xiaoru Guo,[a] Rebecca Tallon,[b] Xingkang Huang[a] and Junhong Chen*[a]

**This work reports on a highly porous N-doped graphene-based capacitive deionization device, which exhibits a high removal efficiency (90–100%), fast removal (<30 min), and good regeneration performance (10 cycles, 99% retention) for multiple heavy metals ($Pb^{2+}$, $Cd^{2+}$, $Cu^{2+}$, $Fe^{2+}$, *etc.*) in water with a wide range of concentrations (0.05–200 ppm).**

A number of methods have been developed to remove heavy metal ions from water, including chemical precipitation, ion-exchange by resin or zeolite, adsorption by carbon, membrane filtration (*e.g.*, reverse osmosis or RO), and electrodialysis (ED).[1–3] However, these conventional methods often suffer from problems of limited efficiency at low metal concentrations, fouling by organic matters, high cost and pressure drop, or low regeneration rates. Alternatively, capacitive deionization (CDI) has emerged as a robust, energy-efficient, and cost-effective competitor to RO and ED, with applications ranging from metal ions removal, water softening, to desalination at a low total dissolved solids (TDS) concentration (<5000 ppm).[3–8] The major market advantages of CDI are (1) low life-cycle cost, (2) ability to remove a wide range of ionic contaminants, (3) high recovery rate (>90%), and (4) low energy consumption.

The CDI technology has been extensively studied for applications of water softening and desalination, including materials innovation (*e.g.*, graphene, carbon nanotube or CNT, mesoporous carbon, metal oxide/carbon),[9] theoretical modeling, architectural optimization,[8] kinetics and mechanism studies,[10] and energy recovery;[10–14] however, CDI for the removal of heavy metals is still in its infancy. So far only a few studies have been reported on the removal of $Cu^{2+}$, $Pb^{2+}$, $As^{3+}$, $Cd^{2+}$, and $Cr^{3+}$ ions using activated carbon cloth (ACC),[15,16] plasma-treated CNTs,[17] carbon aerogel,[18,19] and $TiO_2$/carbon fibers.[20] For example, Huang *et al.* attempted to concurrently remove $Pb^{2+}$, $Cd^{2+}$ and $Cr^{3+}$ using ACC-based CDI, but the removal efficiency can only reach 40–80% even after 2 h (0.05–0.5 mM, 1.2 V).[15] Obviously, it still requires considerable efforts to enhance the metal adsorption capacity, accelerate the removal, and improve the cycling stability. To this end, it is highly desirable to develop new adsorbent materials with the combination of high surface area, porous structure, high conductivity, and good stability.

Graphene, a 2D carbon nanosheet, is of particular interest for CDI because of its outstanding electrical conductivity, superior mechanical flexibility, large surface area, and high thermal-chemical stability. Graphene-based materials, such as hydrogels, sponges, and 3D macroporous structures, have been widely studied for water desalination,[21–25] but seldom for heavy metal removal. On the other hand, the aforementioned graphene materials are prepared by hydrothermal plus freeze drying and microwave or template-assistant methods, which are time-consuming and thus costly. Furthermore, the resulting graphene has a relatively small pore volume. It is hence very necessary to develop a facile and cost-effective method to construct porous graphene with a high pore volume.

Here we report on novel crumpled N-doped graphene (CNG) nanosheets by a facile one-pot method, *i.e.*, thermally treating a mixture of graphene oxide and cyanamide at 900 °C (see experimental in the ESI†). As expected, the as-prepared CNG had a mesoporous structure with a high surface area (695 $m^2\ g^{-1}$), a large pore volume (2.27 $cm^3\ g^{-1}$), and abundant defective sites (Fig. S1, ESI†). This unique CNG was used as electrode material for membrane-CDI to remove multiple heavy metals (*e.g.*, $Pb^{2+}$, $Cd^{2+}$, $Cu^{2+}$, $Ni^{2+}$, $Zn^{2+}$, $Co^{2+}$, $Fe^{2+}$) simultaneously (see the schematic/device in Fig. S2, ESI†). We expect to achieve a high adsorption capacity, high removal efficiency, fast removal, and good cycling performance. To the best of our knowledge, this is the first report on simultaneous removal of multiple heavy metals from water using CNG-based MCDI technology.

Transmission electron microscopy (TEM) and SEM/energy dispersive X-ray spectroscopy (EDS) were conducted to identify the morphology and surface composition of CNG sheets. The TEM image in Fig. 1a clearly shows that CNG has a crumpled

[a] *University of Wisconsin-Milwaukee, Mechanical Engineering Department, Milwaukee, WI, 53211, USA. E-mail: jhchen@uwm.edu*
[b] *A.O. Smith Corporation, Corporate Technology Center, Milwaukee, WI, 53224, USA*

† Electronic supplementary information (ESI) available. See DOI: 10.1039/c6cc08515f

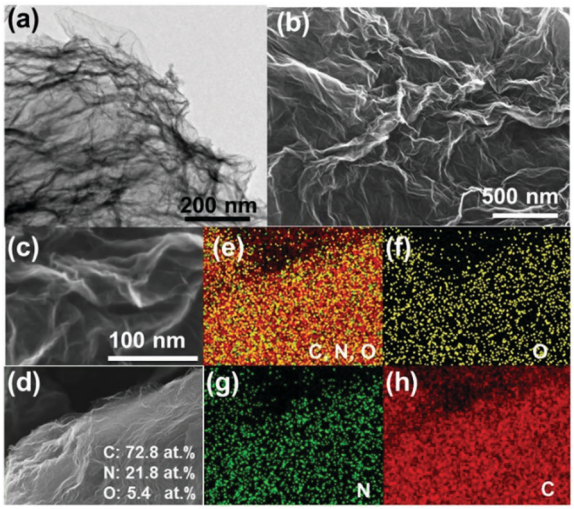


Fig. 1 (a) TEM, (b–d) SEM and (e–h) elemental mapping images for N-doped graphene nanosheets.

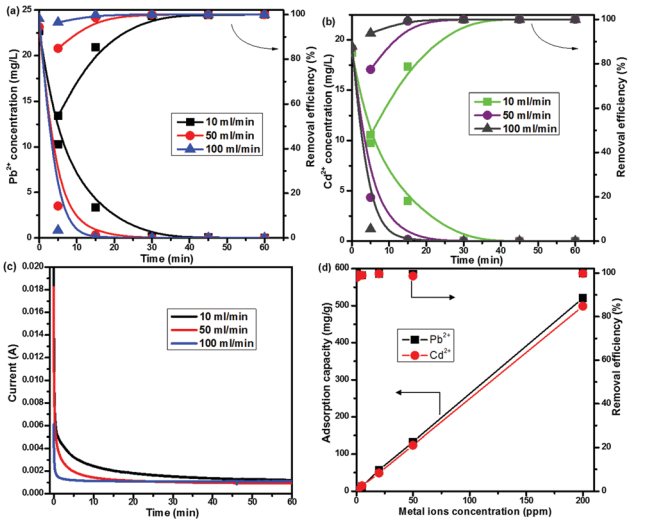


Fig. 2 MCDI performance for (a) $Pb^{2+}$ and (b) $Cd^{2+}$ removal at different flow rates; (c) the corresponding *I–t* curves; and (d) removal efficiency and adsorption capacity of $Pb^{2+}$ and $Cd^{2+}$ at different concentrations (0.05–200 ppm, flow rate: 50 ml $min^{-1}$, 25 mg materials, 50 ml solution, 1.2 V, batch mode).

structure, in which the wrinkles result from the crumpling of graphene sheets rather than from the stacking of graphene. Consistent with $N_2$ sorption analysis (Fig. S3, ESI†), the SEM images in Fig. 1b and c further confirm that totally different from flat GO sheets, CNG has crumpled networks, a rough surface, and a porous structure. The formation of such a porous N-doped structure was because during the *in situ* thermal treatment process, the removal of N-containing polymeric species ($C_3N_3^+$, $C_2N_2^+$) led to the shrinking of flat GO sheets spontaneously.[26] The elemental mapping images (Fig. 1d–h) demonstrate the even distribution of C, N and O elements and the successful doping of N species into the graphene lattice, which could provide more active sites and create more mesopores in the graphene architecture. The content of N species can reach as high as 21.8 at%, again highlighting that for preparation of N-rich porous graphene, our method is simple, facile, and cost-effective without using any surfactants, templates, organic solvents, or post-treatments.

To explore the electro-sorption ability of the CNG electrodes, the potential sweep cyclic voltammetry (CV) was carried out in a three-electrode setup (see details in the ESI†). The CNG electrode showed a typical rectangular shape CV curve at a low scan rate of 25 mV $s^{-1}$ (Fig. S4, ESI†). No oxidation/reduction peaks appeared in the selected potential range (−0.4–0.8 V *vs.* Ag/AgCl), suggesting that the ions were mainly adsorbed on the electrode surface by forming an electrochemical double layer, rather than through electrochemical reduction or oxidation reactions. When varying the scan rates from 25 to 500 mV $s^{-1}$, CV curves still retained the rectangular shapes and were all symmetrical with respect to the *X*-axis, which confirmed that the capacitive processes were highly reversible. In addition, the current values could reach a plateau quickly after reversing the potential sweep, indicating that the ions could adsorb and desorb from the CNG electrode surface quickly and effectively.

The CNG-based MCDI performance for $Pb^{2+}$ and $Cd^{2+}$ removal was evaluated step-by-step by adjusting the conditions: (1) changing the flow rates (10–100 ml $min^{-1}$), (2) varying the ion concentration (0.05–200 ppm), and (3) conducting competitive adsorption of multiple ions. Fig. 2a and b shows the effect of flow rate on the removal of $Pb^{2+}$ and $Cd^{2+}$ starting from ~20 ppm at 1.2 V. It is clear that it took at least 45 min to completely remove both $Pb^{2+}$ and $Cd^{2+}$ at a low flow rate of 10 ml $min^{-1}$. Increasing the flow rate to 100 ml $min^{-1}$ significantly enhanced the efficiency and removal rate. For example, the content of $Pb^{2+}$ dramatically decreased from ~24 ppm to 35 ppb at 15 min and to 0 ppb at 30 min (far below the USA EPA action level of 15 ppb).[27] Even within 5 min the removal efficiency can reach as high as 95%. This is because in a circulating model a high flow rate can facilitate the diffusion of ions within graphene networks and provide more ions for adsorption sites. The *I–t* curves (Fig. 2c) further demonstrate that the current sharply decayed to 0.001 A (in less than 5 min) at 100 ml $min^{-1}$, while it gradually decreased with a tail till 40 min at 10 ml $min^{-1}$, indicating that metal ions can easily access adsorption sites at a high flow rate. Zhao *et al.* also observed that CDI desalination efficiency was enhanced when operated at a high flow rate.[23] Noticeably, the performance of CNG was superior to other ACC, CNT, and carbon aerogel electrode materials for heavy metal removal by CDI reported previously,[4,15,17] which generally showed a low efficiency (<50%) and required a longer duration (>2 h) (Table S1, ESI†). The MCDI performance was also superior to that of the CNG-based CDI (no ion-exchange membrane, IEM), which showed a slower removal rate and lower efficiency (Fig. S5, ESI†). It took 60 min to only reach ~65% removal for $Pb^{2+}$ and ~30% removal for $Cd^{2+}$. Obviously, IEM could significantly facilitate ion transport and minimize the co-ion expulsion effect.

The CNG-based MCDI can also remove $Pb^{2+}$ and $Cd^{2+}$ completely and simultaneously from water with a wide range of initial

concentrations (0.05–200 ppm). For solutions with low initial concentrations (50–500 ppb), $Pb^{2+}$ and $Cd^{2+}$ can be quickly removed within 5 min (Fig. S6a, ESI†). The efficiency can reach almost 100% (Fig. 2d), and the residual $Pb^{2+}$ is below the EPA recommended action level of 15 ppb. This low initial concentration range can mimic the real environmental systems, where large volumes of dilute solution could be treated. For solutions with high concentrations (1–200 ppm), CNG-based MCDI also demonstrated a superior efficiency (100%) to deionize $Pb^{2+}$ and $Cd^{2+}$ from water, while it took a longer duration (at least 30 min) at 200 ppm. This result indicates that our material and device have great potential to treat wastewater containing high concentrations of heavy metals. More importantly, at 200 ppm the adsorption capacity of NG for $Pb^{2+}$ and $Cd^{2+}$ can reach 521 mg $g^{-1}$ and 498 mg $g^{-1}$, respectively. The removal capacity of $Pb^{2+}$ delivered by CNG was at least twice higher than that of graphene-based aerogel, ACC, and CNTs reported previously.[4,15,17] This superior performance is primarily because CNG could provide a large ion-accessible surface area, porous structure for fast ion transport, and highly conductive networks, while N-doping plays a critical role in creating such a unique crumpled structure. N dopants could also change spin density and charge distribution of carbon atoms in the graphene, thereby inducing the formation of surface "activated sites". Such activated sites could participate in the electro-sorption of ions.[28] Noticeably, different from the conventional adsorption process that is usually a time-consuming process (a few hours or longer), the present MCDI not only offers a high removal efficiency and a high capacity, but also achieves a high removal rate.

Besides $Pb^{2+}$ and $Cd^{2+}$, the real water system may contain other interfering cations and anions, such as $Ni^{2+}$, $Co^{2+}$, $Fe^{2+}$, $Cu^{2+}$, $Zn^{2+}$, $Mg^{2+}$, $Ca^{2+}$, $Cl^{-}$, $NO_3^{-}$, and $SO_4^{2-}$. To determine the selectivity of CNG-based MCDI, we conducted competitive adsorption of multiple metal ions using MCDI. Among the various cations (Fig. 3a), $Fe^{2+}$ was most easily removed with a high efficiency and a high rate (~96% at 15 min), while the elimination of $Cd^{2+}$ was the slowest (~80% at 30 min). $Cu^{2+}$ and $Pb^{2+}$ showed a similar removal trend, but their removal efficiency was slightly higher than that of others ($Co^{2+}$, $Ni^{2+}$, $Zn^{2+}$, $Mg^{2+}$ and $Ca^{2+}$). Eventually, the removal efficiency of all the nine cations could reach 90–100% at 45 min. This is an important finding that demonstrates the strong capability of CNG-based MCDI to remove multiple metals efficiently (>90%), quickly (<45 min), and simultaneously. Theoretically, the anions ($Cl^{-}$, $NO_3^{-}$, $SO_4^{2-}$) from metal precursors will also be attracted by the positively charged electrode. In this work, however, the removal of anions was not measured. Our future work will focus on the study of removal of both anions and cations after optimizing the operation conditions.

We also simulated the kinetics of heavy metal sorption using a pseudo first-order kinetic model, following the Langmuir adsorption model. The equation can be expressed as follows:

$$q_t = q_e(1 - e^{-kt})$$

where $q_t$ and $q_e$ are the adsorption amount (mg $g^{-1}$) at time $t$ and at equilibrium, and $k$ is the rate constant ($min^{-1}$). As shown in Fig. 3b, $Fe^{2+}$ shows the highest rate constant (0.232 $min^{-1}$), over 100% and six times higher than that of $Pb^{2+}$ (0.077 $min^{-1}$), $Cu^{2+}$ (0.089 $min^{-1}$) and $Cd^{2+}$ (0.031 $min^{-1}$), respectively. During the MCDI process, the electrostatic attraction should dominate the adsorption of metals. However, from Fig. 3 one can find that the removal efficiency and rate constant are different for the different types of ions at the initial 25 min. This difference may be caused by the surface functional groups of CNG (–OH, –COOH) and metal ion properties (radius, ionic potential, hydrated radius and charge size).[15,29] The high efficiency and rate for $Fe^{2+}$ is because $Fe^{2+}$ could be easily oxidized to $Fe^{3+}$, which has a higher charge size and stronger affinity to surface OH groups than other ions. In this case, Fe ions have a preference to occupy the adsorption sites even in the presence of other competitive ions. The least favorable adsorption for $Cd^{2+}$ is mainly due to its larger hydrated radius and expulsion effect by competitors,[29] consistent with the literature reports that $Cd^{2+}$ showed a lower efficiency than $Pb^{2+}$ and $Cr^{3+}$.[15] Among the mixed ions, $Pb^{2+}$ has the largest ionic radius (1.32 Å) and atomic weight (207) and larger electronegativity (2.33), which can contribute to its favorable adsorption, while $Cu^{2+}$ has a stronger affinity to complex with hydroxyl groups. Obviously, there is a trade-off among the above-mentioned factors, which may have a combined effect on the adsorption process, thereby leading to a comparable efficiency and rate constant between $Cu^{2+}$ and $Pb^{2+}$ but higher than those of others like $Zn^{2+}$, $Co^{2+}$, $Ni^{2+}$ and $Cd^{2+}$.

A good regeneration performance of CNG is quite important for heavy metal removal. Fig. 4a shows the removal efficiency of $Pb^{2+}$ and $Cd^{2+}$ during the first 10 cycles, which were conducted by repeating adsorption (charging at 1.2 V) and desorption (discharging at 0 V) processes in a $Pb^{2+}$ + $Cd^{2+}$ solution. It is clearly seen that at each cycle, the efficiency for $Pb^{2+}$ and $Cd^{2+}$ remained at ~100%, suggesting that the CNG electrodes can be completely regenerated and reused over 10 cycles without any significant degradation. More importantly, the regeneration process is facile and eco-friendly without any acid washing or post treatment process. The *I*–*t* curves during the charge–discharge process further demonstrate that CNG-based MCDI has an outstanding recovery rate and reversibility (Fig. 4b). The charge–discharge process in one cycle only takes ~30 min. This good performance (high retention efficiency (99%) and

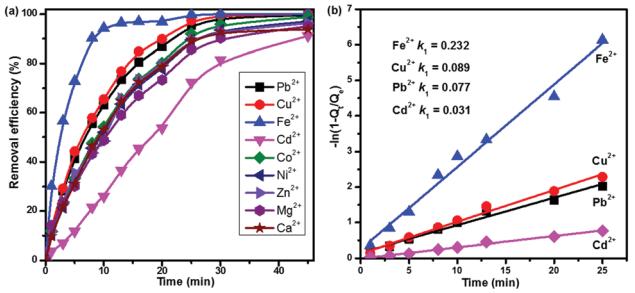


Fig. 3 MCDI performance for multiple ions removal: (a) time-dependent efficiency and (b) kinetics for $Fe^{2+}$, $Cu^{2+}$, $Pb^{2+}$, and $Cd^{2+}$ (~10 ppm for each metal ion, flow rate: 50 ml $min^{-1}$, 25 mg materials, 100 ml solution, 1.2 V).

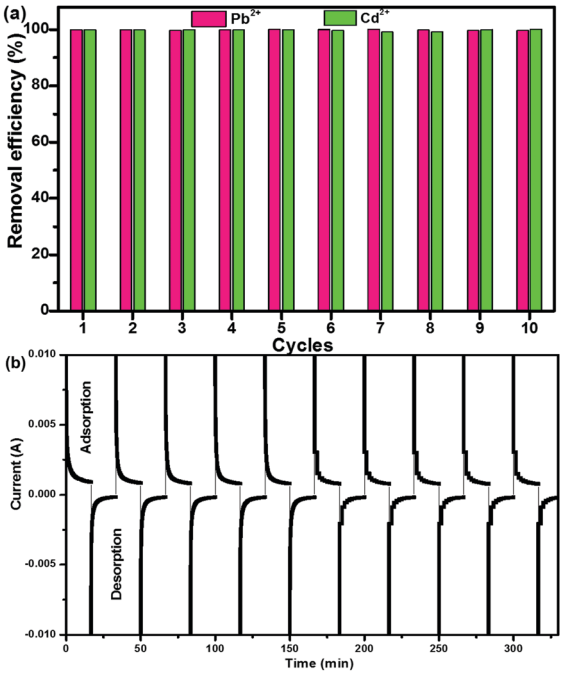


Fig. 4 (a) The removal efficiency of $Pb^{2+}$ (pink bar) and $Cd^{2+}$ (green bar) during 10 cycles. The efficiency is calculated on the basis of concentration after 15 min adsorption; at the end of each cycle, the electrode materials were regenerated by discharging at 0 V. Fresh feeding water (50 ml, ~20 ppm $Pb^{2+}$ + $Cd^{2+}$) was then introduced to replace the original solution; and (b) the *I*–*t* curves of adsorption (charge at 1.2 V) and desorption (discharge at 0 V) over 10 cycles.

high regeneration rate) may result from the unique porous structure of crumpled NG networks and application of ion-exchange membranes that facilitate ion transport, minimize the co-ion expulsion effect, and enhance the charge efficiency. The superior recycling performance and stability indicate the promise of CNG MCDI for water purification.

In summary, we have developed a facile one-pot method to construct a highly porous N-doped graphene with a high surface area and a large pore volume. The resulting CNG was used as the electrode material for MCDI to remove multiple heavy metals from water. The CNG-based MCDI demonstrated a high removal efficiency (90–100%), a high removal rate (<30 min), a high capacity (~500 mg $g^{-1}$) and a good recycling performance (10 cycles, 99% retention) to remove $Pb^{2+}$ and $Cd^{2+}$ simultaneously from water with a wide range of concentrations (0.05–200 ppm). More importantly, the CNG-based MCDI also has a strong capability to remove multiple metals efficiently, concurrently and quickly (>90% within 45 min). The findings reported in this work shed light on the application of CNG-based MCDI for water purification and softening, which can potentially compensate the current technologies for heavy metal removal.

The ion exchange membrane used to assemble the CDI device was provided by Pentair.

## Notes and references

1 F. L. Fu and Q. Wang, *J. Environ. Manage.*, 2011, **92**, 407–418.
2 M. Hua, S. J. Zhang, B. C. Pan, W. M. Zhang, L. Lv and Q. X. Zhang, *J. Hazard. Mater.*, 2012, **211**, 317–331.
3 I. Duru, D. Ege and A. R. Kamali, *J. Mater. Sci.*, 2016, **51**, 6097–6116.
4 X. Gu, Y. Yang, Y. Hu, M. Hu and C. Wang, *ACS Sustainable Chem. Eng.*, 2015, **3**, 1056–1065.
5 T. Humplik, J. Lee, S. C. O'Hern, B. A. Fellman, M. A. Baig, S. F. Hassan, M. A. Atieh, F. Rahman, T. Laoui, R. Karnik and E. N. Wang, *Nanotechnology*, 2011, **22**, 292001.
6 S. Porada, R. Zhao, A. van der Wal, V. Presser and P. M. Biesheuvel, *Prog. Mater. Sci.*, 2013, **58**, 1388–1442.
7 F. A. AlMarzooqi, A. A. Al Ghaferi, I. Saadat and N. Hilal, *Desalination*, 2014, **342**, 3–15.
8 M. E. Suss, S. Porada, X. Sun, P. M. Biesheuvel, J. Yoon and V. Presser, *Energy Environ. Sci.*, 2015, **8**, 2296–2319.
9 S. Daer, J. Kharraz, A. Giwa and S. W. Hasan, *Desalination*, 2015, **367**, 37–48.
10 F. Duan, Y. Li, H. Cao, Y. Xie and Y. Zhang, *Desalin. Water Treat.*, 2014, **52**, 1388–1395.
11 Y. Zhao, Y. Wang, R. Wang, Y. Wu, S. Xu and J. Wang, *Desalination*, 2013, **324**, 127–133.
12 M. A. Anderson, A. L. Cudero and J. Palma, *Electrochim. Acta*, 2010, **55**, 3845–3856.
13 R. Zhao, P. M. Biesheuvel and A. van der Wal, *Energy Environ. Sci.*, 2012, **5**, 9520–9527.
14 P. Dlugolecki and A. van der Wal, *Environ. Sci. Technol.*, 2013, **47**, 4904–4910.
15 Z. Huang, L. Lu, Z. X. Cai and Z. J. Ren, *J. Hazard. Mater.*, 2016, **302**, 323–331.
16 C. S. Fan, S. C. Tseng, K. C. Li and C. H. Hou, *J. Hazard. Mater.*, 2016, **312**, 208–215.
17 L. F. Yang, Z. Shi and W. H. Yang, *Surf. Coat. Technol.*, 2014, **251**, 122–127.
18 X. Y. Gu, Y. Yang, Y. Hu, M. Hu and C. Y. Wang, *ACS Sustainable Chem. Eng.*, 2015, **3**, 1056–1065.
19 Z. Wang, L. Yue, Z. T. Liu, Z. H. Liu and Z. P. Hao, *J. Mater. Chem.*, 2012, **22**, 14101–14107.
20 L. Peng, Y. P. Chen, H. Dong, Q. R. Zeng, H. J. Song, L. Y. Chai and J. D. Gu, *Water, Air, Soil Pollut.*, 2015, **226**, 203.
21 Y. Liu, T. Chen, T. Lu, Z. Sun, D. H. C. Chua and L. Pan, *Electrochim. Acta*, 2015, **158**, 403–409.
22 Y. Liu, X. Xu, M. Wang, T. Lu, Z. Sun and L. Pan, *J. Mater. Chem. A*, 2015, **3**, 17304–17311.
23 S. S. Zhao, T. T. Yan, H. Wang, G. R. Chen, L. Huang, J. P. Zhang, L. Y. Shi and D. S. Zhang, *Appl. Surf. Sci.*, 2016, **369**, 460–469.
24 Z.-Y. Yang, L.-J. Jin, G.-Q. Lu, Q.-Q. Xiao, Y.-X. Zhang, L. Jing, X.-X. Zhang, Y.-M. Yan and K.-N. Sun, *Adv. Funct. Mater.*, 2014, **24**, 3917–3925.
25 X. Xu, Y. Liu, T. Lu, Z. Sun, D. H. C. Chua and L. Pan, *J. Mater. Chem. A*, 2015, **3**, 13418–13425.
26 L. Liu, X. Huang, X. Guo, S. Mao and J. Chen, *J. Power Sources*, 2016, **328**, 482–491.
27 I. R. Pala and S. L. Brock, *ACS Appl. Mater. Interfaces*, 2012, **4**, 2160–2167.
28 G. A. Ahmad Amiri, M. Shanbedi, M. Savari, S. N. Kazi and B. T. Chew, *Sci. Rep.*, 2015, 17503.
29 Y. Ding, Y. G. Liu, S. B. Liu, Z. W. Li, X. F. Tan, X. X. Huang, G. M. Zeng, Y. Y. Zhou, B. H. Zheng and X. X. Cai, *RSC Adv.*, 2016, **6**, 5223–5232.

 